Case Report

Radiation-induced vascular malformations in the brain, mimicking tumor in MRI-based treatment response assessment maps (TRAMs)

David Guez [a,*], David Last [a], Dianne Daniels [a], Shirley Sharabi [a], Dvora Nass [b,c], Ouzi Nissim [d], Roberto Spiegelmann [d,c], Galia Tzarfaty [e,c], Chen Hoffmann [e,c], Alisa Talianski [f,c], Yigal Shoshan [g], Yakov Fellig [h], Sagi Harnof [i,c], Zvi R. Cohen [d,c], Leor Zach [f,c], Yael Mardor [a,c]

[a] Advanced Technology Center, Sheba Medical Center, Ramat-Gan 52621, Israel
[b] Pathology Institute, Sheba Medical Center, Ramat-Gan 52621, Israel
[c] Sackler Faculty of Medicine, Tel-Aviv University, Tel-Aviv 69978, Israel
[d] Neurosurgery Dept, Sheba Medical Center, Ramat-Gan 52621, Israel
[e] Radiology Institute, Sheba Medical Center, Ramat-Gan 52621, Israel
[f] Oncology Institute, Sheba Medical Center, Ramat-Gan 52621, Israel
[g] Neurosurgery Dept., Hadassah Medical Center, Jerusalem 91120, Israel
[h] Pathology Inst., Hadassah Medical Center, Jerusalem 91120, Israel
[i] Neurosurgery Dept., Rabin Medical Center, Petach Tikva 49100, Israel

A R T I C L E   I N F O

1. Introduction

Previous studies suggest that 14–30% of glioblastoma multiforme (GBM) patients and 5–24% of patients with brain metastases demonstrate imaging treatment-effects in the first few months after treatment [1–3]. These treatment-induced imaging changes, often termed pseudoprogression/radiation-necrosis, are depicted as increasing volumes of contrast-enhancing lesions on MRI, mimicking progression. Therefore, treatment decisions, such as whether to operate on a patient with radiographic deterioration, continue current treatment or change treatment is a daily unsolved struggle.

In addition, radiation-based treatments may also induce vascular malformations such as radiation-induced Cavernous malformations (RICM) and capillary telangiectasias. Cavernous malformations are low-flow vascular malformations, characterized by the lack of mural elements of mature vascular structures and intervening parenchymal neural tissue [4]. Radiation induced capillary telangiectasias (RIT), thin-walled ectatic capillaries with intervening normal brain parenchyma, usually occur 3–9 months after irradiation. Cavernomas take a longer time to develop (1–35 years) after radiation [5].

RICMs mostly develop in the pediatric population [6], but are also observed in adults. In a literature search from 2006 by Nimjee et al [7], 76 cases of RICMs were found. A retrospective study conducted at Mayo clinic found 32 RICMs [5]. RICMs latency median was 12.0 years with only 3 diagnosed in the first two years post radiation (9.3%). Kleinschmidt-DeMasters and Lillehei [8] found 13 cases between 2000 and 2016 in their surgical neuropathology databases. The latency median was 18 years. Strenger et al calculated a cumulative index of 2.24%, 3.86%, 4.95%, and 6.74% at 5, 10, 15, and 20 years following radiotherapy of children,

respectively [9]. Vinchon et al [10] identified cumulative indices for their cohort in children at 10 years of 8.9%. Although RICMs are rare in adults with astrocytoma, mainly due to poor survival, three cases of long term survivals were reported in the literature to develop RICMs 10, 19 and 26 years post radiotherapy [11]. Gaensler and colleagues reported a series of 20 patients with RITs (6 proven pathologically) for whom the latency was only 2.7 years [12]. 70% of the 20 patients were <20 years old.

The diagnosis of RICM and RIT is mainly done by MRI. Imaging typically reveals an enhancing multiloculated cystic lesion with popcorn- or mulberry-like features on both T1- and T2-weighted images. Although the radiological appearances of RICMs/RITs are often similar to non-radiation Cavernomas, RICMs sometimes show mixed intensity with an enhancing cystic and/or solid component and an incomplete hemosiderin rim [6].

We have recently presented the application of delayed-contrast MRI for calculating high resolution treatment assessment response maps (TRAMs) showing clear differentiation between tumor/non-tumor tissues in brain tumor patients [13–15]. This methodology is based on MRIs acquired 5 min and >1 h (60–105 min) after a conventional injection of contrast agent. Blue/tumor regions in the TRAMs represent efficient clearance of contrast from the tissue (delayed signal < early signal) while red/non-tumor regions in the TRAMs represent contrast accumulation (delayed signal > early signal). The TRAMs were validated histologically in 51 resected lesions from patients with primary and metastatic brain tumors reaching 92% positive predictive value (PPV) and 100% sensitivity to morphologically active tumor. When studying the histological samples, we found that the common vessels morphology in the blue regions was undamaged vessels lumens, while vessels in the red regions presented different stages of vessel necrosis. Therefore, one explanation for the difference between the two populations may be that vessels in blue/tumor regions provide efficient contrast clearance from the tissue, while the damaged lumens in the red/treatment-effects regions are unable to clear the accumulating contrast, resulting in contrast accumulation.

Over 400 adult patients have been recruited thus far to our ongoing TRAMs-based studies in Israel since 2010. As the TRAMs cannot differentiate blood vessels from active tumor (both appearing blue), we studied here whether RCIMs/RITs may mimic tumors in the TRAMs.

2. Materials and methods

2.1. Patients and treatments

Patients with space occupying lesions in the brain, including primary or metastatic brain tumors post treatment were recruited to two ongoing exploratory trials designed to study the application of the TRAMs for differentiating active tumor from treatment effects. The studies were conducted after approval of the local ethics committee at Sheba Medical Center. Written informed consent was obtained from all patients.

From these studies, a total of 99 histological samples were available, and cases in which the pre-surgical TRAMs were found false-positive for tumor were re-reviewed in an attempt to provide a possible explanation for the efficient contrast-clearance depicted in the TRAMs. For comparison, patients with newly diagnosed cavernomas and patients with treated arteriovenous malformations (AVMs) were studied as well. One of the AVMs was biopsied.

2.2. MRI – data acquisition

Patients were scanned by MRI immediately following recruitment and every 2 months thereafter or earlier according to their clinical condition. The MRIs were acquired using 1.5T/3T General Electric MRI systems (GE Medical Systems, Waukesha, WI, USA) and included DSC, Fast spin-echo T2-weighted, Gradient Echo T2*, T2 FLAIR and echo-planar diffusion-weighted MRI. Three high resolution 3D FSPGR T1-weighted MRIs (T1-MRIs) were acquired before, 5 min and 60–105 min after contrast injection ($1 \times 1 \times 1$ mm resolution, repetition time of 2.9 ms, bandwidth of 244 Hz, 20° flip angle, 256×256 acquisition matrix, 400 ms inversion time).

A standard single dose (0.2 ml/Kg, 0.1 mmol/kg) of Gd-DOTA (Dotarem, 0.5 mmol/mL, Guerbet, 95,943 Roissy CdG Cedex, France) was injected intravenously using an automatic injection system.

2.3. MRI – data analysis

All image analysis was performed using MatLab (version R2010a, The MathWorks, Inc. Natick, MA, US).

The TRAMs were calculated by subtracting T1-MRIs acquired 5 min post-contrast from those acquired >1 h post-contrast. These maps depict spatial distribution of contrast accumulation/clearance. For example, in case of normal blood vessels, due to contrast clearance from the blood, the signal decreases with time; therefore, the subtraction maps show negative values (blue in the maps). In case of contrast accumulation, the maps show positive values (red).

In order to increase the sensitivity to small changes it was essential to perform image pre-processing consisting of corrections for intensity variations and whole body image registration as previously described [13].

2.4. Histology

Comparison between the pre-surgical maps and histology for patients participating in our studies during 2010–2014 was previously reported for 51 lesions obtained from patients with brain tumors [13,14]. Here we report cases of patients resected during 2010–2017, which showed no active tumor in histology despite significant blue regions in the pre-surgical TRAMs.

3. Results

Five lesions resected from 4 patients with previously treated brain tumors, showing significant blue regions in the pre-surgical TRAMs and vascular malformations with no active tumor in histology, were found.

For comparison, two patients with newly diagnosed cavernomas and three with treated AVMs were scanned by the TRAMs as well. One of the AVMs was biopsied.

3.1. Detailed description of the findings – patients with brain tumors

3.1.1. Patient #1

TRAMs were acquired 15 months after SRS (18 Gy) to a 6×5 mm brain metastasis (left frontal) of breast carcinoma. The pre-surgical TRAMs showed a thin blue rim surrounding a red region. Histology revealed papillary vascular proliferation forming a "Mason tumor" on the borders of a central region of radiation necrosis.

3.1.2. Patient #2

TRAMs were acquired 22 months after gross total resection of GBM followed by standard chemoradiation, and 11 months after initiation of Rindopepimut + TMZ. The pre-surgical TRAMs showed a 2×3 mm blue lesion in the previous surgery site, surrounded by a thin blue rim. Histology revealed RICM (Fig. 1).
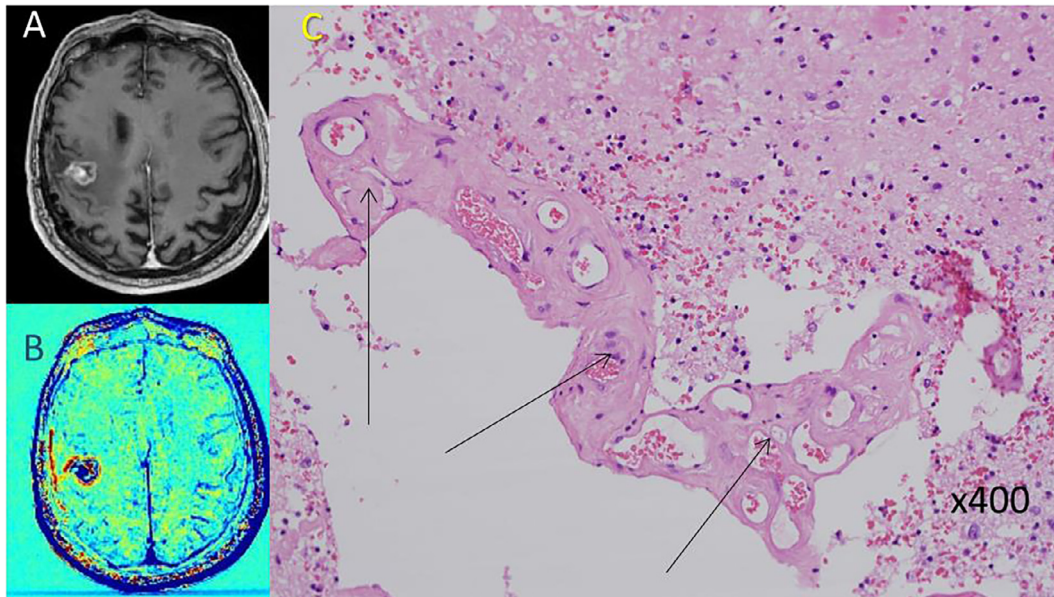
Fig. 1. An example of radiation-induced vascular malformation in a patient with GBM post treatment (patient #2). A, B: Pre-surgical contrast-enhanced T1-weighted MRI and the calculated TRAMs depicting a small blue mass within a surrounding thin blue rim. C: H&E stained paraffin section showing radiation-induced cavernoma-like vascular malformation (arrows). (For interpretation of the references to colour in this figure legend, the reader is referred to the web version of this article.)
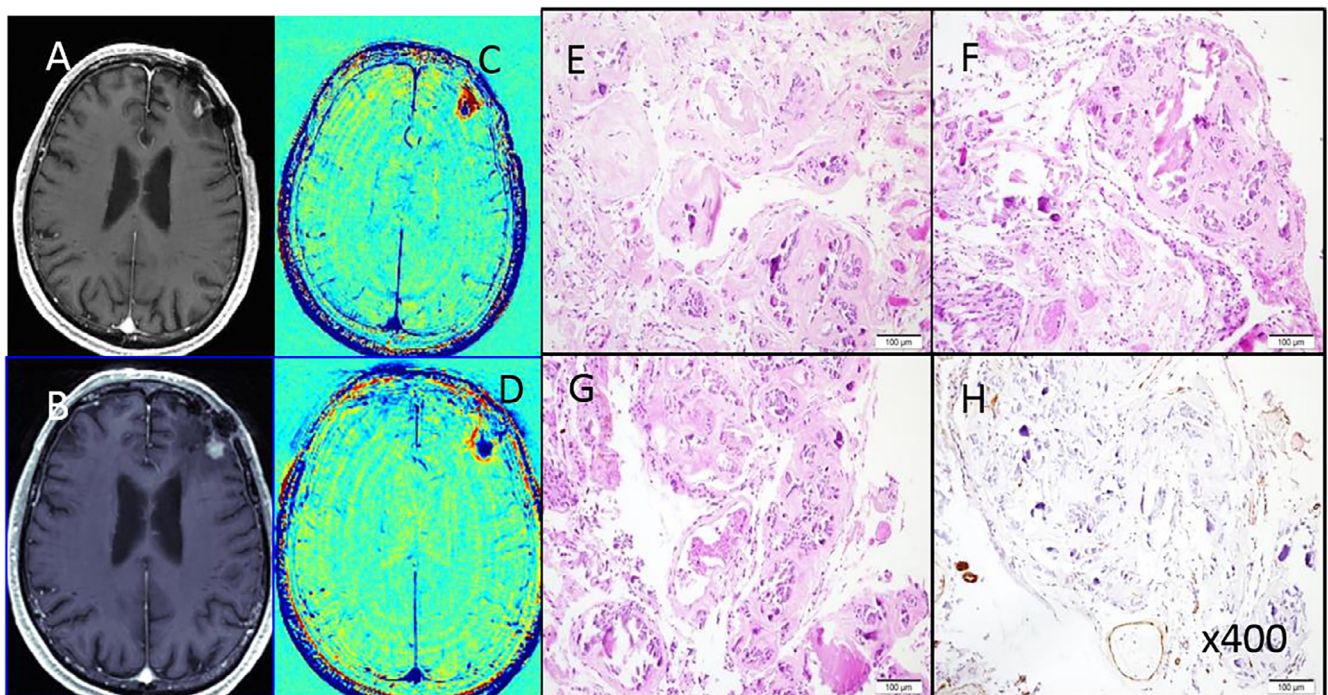

Fig. 2. An example of radiation-induced vascular malformation in a patient with a non-small cell lung cancer brain metastasis post treatment (patient #3). A, C: Pre-surgical contrast-enhanced T1-weighted MRI and the calculated TRAMs depicting a small blue mass on the border of the previous surgery site 29 months post SRS. B, D: Pre-surgical contrast-enhanced T1-weighted MRI and the calculated TRAMs depicting a small blue mass re-growing on the border of the previous surgery site 23 months post removal of the previous lesion and FSR. E–H H&E stained paraffin sections showing cavernoma-like vascular malformations, with back to back vascular channels, marked hyalinization and calcification. H: Immuno-histochemical staining for smooth muscle alpha-actin (SMA) showing only patchy immuno-reactivity in vessel walls, with near-absence in areas. (For interpretation of the references to colour in this figure legend, the reader is referred to the web version of this article.)

3.1.3. Patient #3

TRAMs were acquired 21 months after SRS given to the surgery site of a resected NSCLC brain metastasis, showing a 2–3 mm blue lesion growing in the previous surgery site, surrounded by a thin blue rim. Histology revealed radiation-induced injury and RICM.

The patient was rescanned 8 months after the second surgery. The TRAMs showed an 8 mm blue lesion on the border of the previous surgery site. The patient underwent an additional resection and histology showed again radiation-induced injury and RICM (Fig. 2).
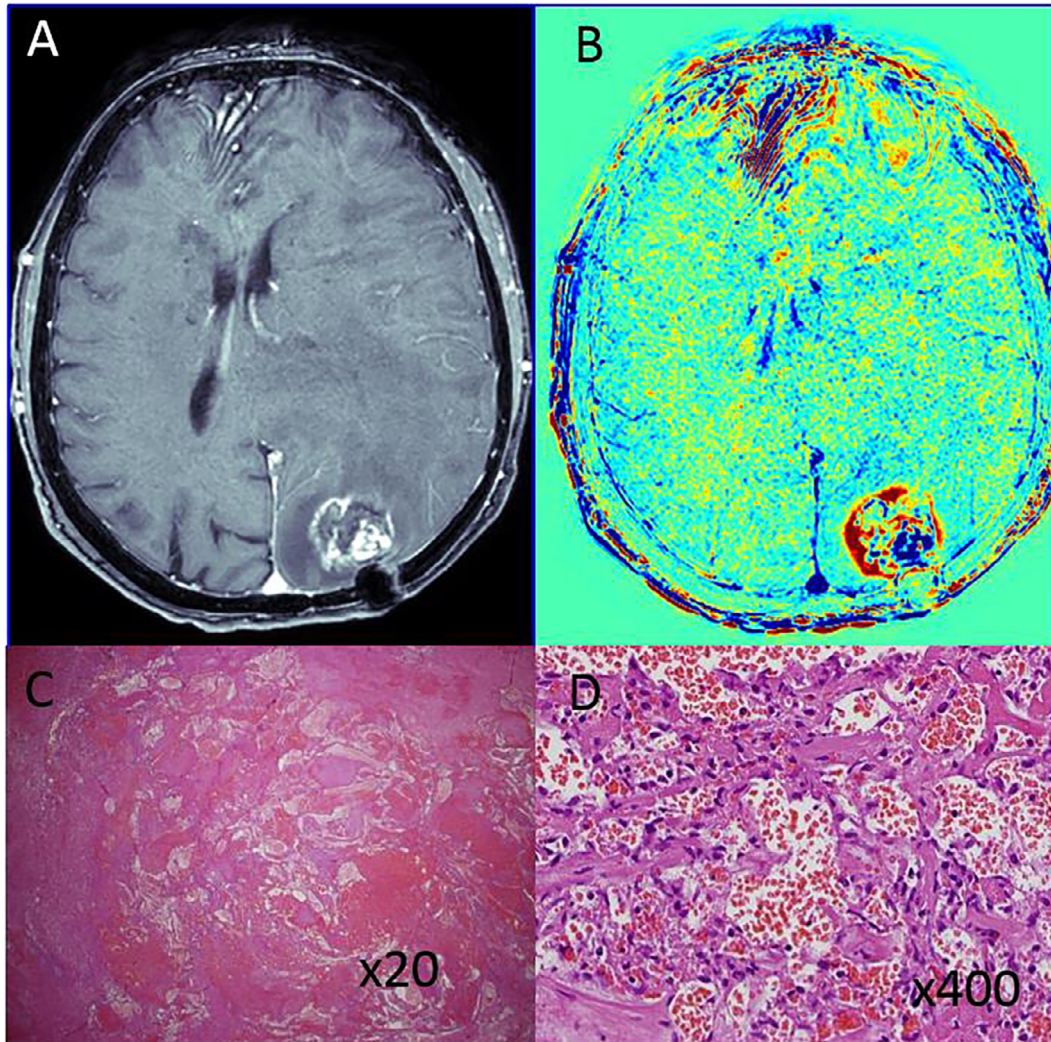
Fig. 3. An example of radiation-induced vascular malformation in a patient with GBM post treatment (patient #4). A, B: Pre-surgical contrast-enhanced T1-weighted MRI and the calculated TRAMs depicting a small blue mass within a surrounding thin blue rim. C, D: H&E stained paraffin section showing radiation-induced cavernoma-like vascular malformation. (For interpretation of the references to colour in this figure legend, the reader is referred to the web version of this article.)
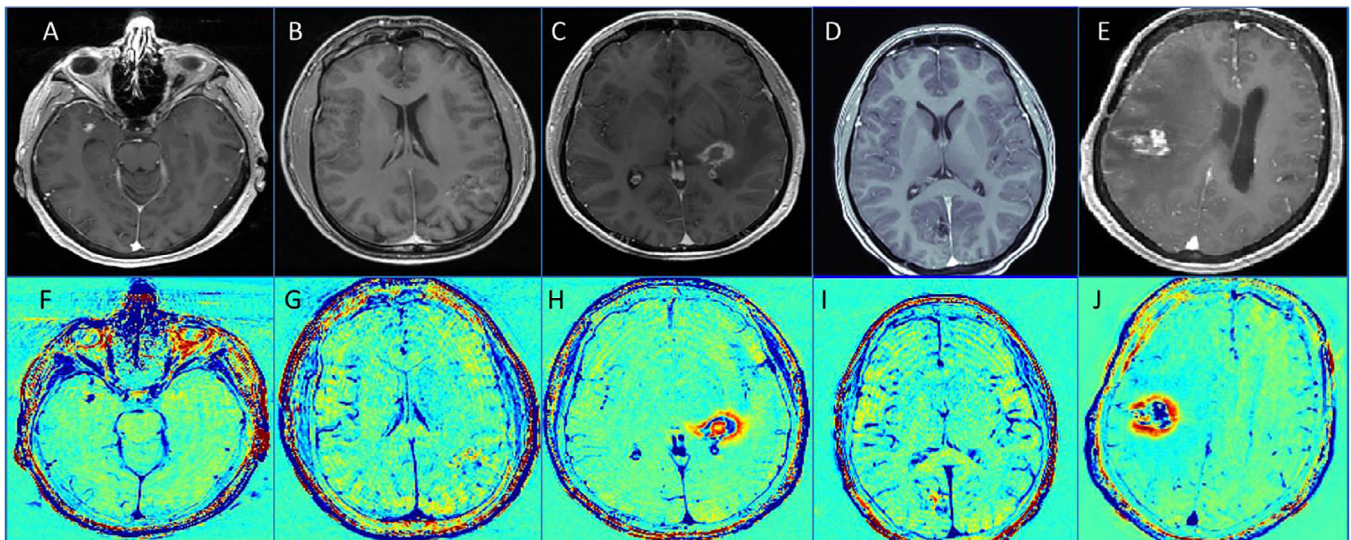

Fig. 4. MRI of the patient 5–9 (patients with treated AVM). A–E: T1 of the five patients. F–J: TRAMs of the five patients.

3.1.4. Patient #4

TRAMs were acquired 23 months after FST to the surgery site of a resected cervical adenocarcinoma brain metastasis (parieto occipital). This was a second resection, performed 17 months after the first. The pre-surgical TRAMs showed a ~1 cm blue lesion surrounded by a larger red region. Histology revealed a large, ~1 cm, RICM (Fig. 3).

3.2. Detailed description of the findings – patients with newly diagnosed cavernomas

3.2.1. Patient #5

TRAMs were acquired 27 months after being diagnosed with cavernoma, showing a 2–3 mm blue lesion (Fig. 4).

3.2.2. Patient #6

TRAMs were acquired 2 months after being diagnosed with cavernoma, showing a region of 2–3 cm in diameter covered with patchy blue lesions (Fig. 4).

3.3. Detailed description of the findings – patients with treated AVMs

3.3.1. Patient #7

TRAMs were acquired 10 months after SRS to a newly diagnosed AVM, showing a non-symmetric thick blue rim within a larger red region (Fig. 4).

3.3.2. Patient #8

TRAMs were acquired one week before SRS to an AVM treated by partial embolization, showing a 3 cm lesion with blue and red components, slightly enhanced on the contrast enhanced T1-MRI (Fig. 4).

3.3.3. Patient #9

TRAMs were acquired with a diagnosis of systemic lymphoma and 5 years after SRS to a newly diagnosed AVM, showing mixed blue and red regions. Cerebral angiogram showed the AVM was closed. A biopsy obtained 3 weeks later showed post-radiation changes and large hyalinized blood vessels of irregular shape with almost complete obliteration of lumens and secondary lumen formation (Fig. 4).

4. Discussion

Not much literature is available concerning the prevalence of radiation-induced vascular malformations after brain tumor treatment. In this study, we screened our database of ~400 patients with primary or secondary brain tumors post treatment, recruited to our TRAMs-related studies since 2010, and found 5 lesions with histologically confirmed radiation-induced vascular malformations after brain tumor irradiation. As only those patients with available histological confirmation have been included (99 histological samples), it may be that the number of cases is actually higher. The small number of cases found, however, suggests that the rate of RCIMs/RITs found in our study is in the order of a few percent of the treated tumors, in line with other published studies [5,7]. As previously published, the PPV of the TRAMs to active tumor was determined histologically to be 93% [14]. These rare cases of lesions appearing blue in the TRAMs and found histologically to consist of radiation-induced vascular malformations, may explain some of the false negative cases leading to this number.

Both active tumors and radiation-induced vascular malformations are depicted in the TRAMs as blue masses, associated with enhancing lesions on contrast-enhanced T1-weighted MRI. In the malformation cases, the lesions were depicted with uniform blue shading in the TRAMs and well delineated borders. This is true for many of the active tumors as well. Therefore, as of yet, the TRAMs are unable to differentiate the five vascular malformations found in our cohort from active brain tumors.

MRI sequences with highest sensitivity to hemosiderin susceptibility effect are more accurate in depicting hemosiderin deposits in the lesions. The most used ones are gradient-echo imaging (GE) and susceptibility-weighted imaging (SWI) sequences [4].

For this reason, we recommend adding to the scanning protocol additional sequences which are sensitive to the hemosiderin susceptibility effect, especially in cases where RICM or RIT are suspected, such as gradient echo MRI or susceptibility-weighted MRI. Still, these sequences are not efficient in differentiating hemorrhages, which are frequent in these patients, from vascular malformations, and may not show any signal in the vicinity of metal subjects such as surgical screws etc.

In conclusion, while the TRAMs are highly effectives to separate between treatment effects and active tumors, it cannot address the specific case of RICM and RIT. The total number of such case are most likely not exceeding a few percent of the cases but other sequences such as SWI are still important to help detecting RICM and RIT.

References

[1] Brandsma D, Van Den Bent MJ. Pseudoprogression and pseudoresponse in the treatment of gliomas. Curr Opin Neurol 2009;22(6):633–8.
[2] Chamberlain MC, Glantz MJ, Chalmers L, Van Horn A, Sloan AE. Early necrosis following concurrent Temodar and radiotherapy in patients with glioblastoma. J Neurooncol 2007;82(1):81–3.
[3] De Wit MCY, De Bruin HG, Eijkenboom W, Sillevis Smitt PAE, Van Den Bent MJ. Immediate post-radiotherapy changes in malignant glioma can mimic tumor progression. Neurology 2004;63(3):535–7.
[4] Wang KY, Idowu OR, Lin DDM. Radiology and imaging for cavernous malformations. Handb Clin Neurol 2017;143:249–66.
[5] Cutsforth-Gregory JK, Lanzino G, Link MJ, Brown RD. Characterization of radiation-induced cavernous malformations and comparison with a nonradiation cavernous malformation cohort. J Neurosurg 2015;122(5):1214–22.
[6] Cha YJ, Nahm JH, Ko JE, Shin HJ, Chang JH, Cho NH, et al. Pathological evaluation of radiation-induced vascular lesions of the brain: distinct from de novo cavernous hemangioma. Yonsei Med J 2015;56(6):1714–20.
[7] Nimjee SM, Powers CJ, Bulsara KR. Review of the literature on de novo formation of cavernous malformations of the central nervous system after radiation therapy. Neurosurg Focus 2006;21(1):e4.

[8] Kleinschmidt-DeMasters BK, Lillehei KO. Radiation-induced cerebral vascular 'malformations' at biopsy. J Neuropathol Exp Neurol 2016;75(11):1081–92.

[9] Strenger V, Sovinz P, Lackner H, Dornbusch HJ, Lingitz H, Eder HG, et al. Intracerebral cavernous hemangioma after cranial irradiation in childhood: incidence and risk factors. Strahlentherapie und Onkol 2008;184(5):276–80.

[10] Vinchon M, Leblond P, Caron S, Delestret I, Baroncini M, Coche B. Radiation-induced tumors in children irradiated for brain tumor: a longitudinal study. Child's Nerv Syst 2011;27(3):445–53.

[11] Fukushima S, Narita Y, Miyakita Y, Ohno M, Takizawa T, Takusagawa Y, et al. A case of more than 20 years survival with glioblastoma, and development of cavernous angioma as a delayed complication of radiotherapy. Neuropathology 2013;33(5):576–81.

[12] Gaensler EH, Dillon WP, Edwards MS, Larson DA, Rosenau W, Wilson CB. Radiation-induced telangiectasia in the brain simulates cryptic vascular malformations at MR imaging. Radiology 1994;193(3):629–36.

[13] Zach L, Guez D, Last D, Daniels D, Grober Y, Nissim O, et al. Delayed contrast extravasation MRI for depicting tumor and non-tumoral tissues in primary and metastatic brain tumors. PLoS ONE 2012;7(12). e52008.

[14] Zach L, Guez D, Last D, Daniels D, Grober Y, Nissim O, et al. Delayed contrast extravasation MRI: a new paradigm in neuro-oncology. Neuro Oncol 2014:1–8.

[15] Daniels D, Guez D, Last D, Hoffmann C, Nass D, Talianski A, et al. Early biomarkers from conventional and delayed-contrast MRI to predict the response to bevacizumab in recurrent high-grade gliomas. Am J Neuroradiol 2016;37(11):2003–9.